

---

# Hessian-Free Laplace in Bayesian Deep Learning

---

James McInerney<sup>1</sup> Nathan Kallus<sup>2,1</sup>

## Abstract

The Laplace approximation (LA) of the Bayesian posterior is a Gaussian distribution centered at the maximum *a posteriori* estimate. Its appeal in Bayesian deep learning stems from the ability to quantify uncertainty post-hoc (i.e., after standard network parameter optimization), the ease of sampling from the approximate posterior, and the analytic form of model evidence. However, an important computational bottleneck of LA is the necessary step of calculating and inverting the Hessian matrix of the log posterior. The Hessian may be approximated in a variety of ways, with quality varying with a number of factors including the network, dataset, and inference task. In this paper, we propose an alternative framework that sidesteps Hessian calculation and inversion. The *Hessian-free Laplace* (HFL) approximation uses curvature of both the log posterior and network prediction to estimate its variance. Only two point estimates are needed: the standard maximum *a posteriori* parameter and the optimal parameter under a loss regularized by the network prediction. We show that, under standard assumptions of LA in Bayesian deep learning, HFL targets the same variance as LA, and can be efficiently amortized in a pre-trained network. Experiments demonstrate comparable performance to that of exact and approximate Hessians, with excellent coverage for in-between uncertainty.

## 1. Introduction

Bayesian neural networks, where a prior is placed on model weights, offer an opportunity to understand uncertainty and direct experimentation. However, exact computation of the model-weight posterior and predictive distributions is prohibitive given size and complexity. It is instead appealing to approximate it using the maximum *a posteriori* (MAP) solu-

tion and the curvature thereof. However, even this curvature, characterized by a Hessian, can be challenging to compute.

Consider the maximum *a posteriori* (MAP) solution of a Bayesian neural network  $f_\theta$  with parameters  $\theta$  given data  $\{(x_i, y_i)\}_{i=1}^n$ ,

$$\hat{\theta} = \arg_{\theta} \max \mathcal{L}_\theta \quad (1)$$

$$\text{where } \mathcal{L}_\theta = \sum_{i=1}^n \log p(y_i | f_\theta(x_i)) + \log p(\theta), \quad (2)$$

for some observation likelihood  $p(y | \phi)$  and prior  $p(\theta)$ . This is equivalent to optimizing a loss (e.g., squared loss for Gaussian likelihood or cross-entropy for categorical likelihood) regularized by  $\log p(\theta)$  and means that computing the MAP of a Bayesian neural network is akin to fitting a vanilla neural network.

As detailed in the next section, the Laplace approximation of the posterior distribution leverages the (negative) Hessian of the log joint distribution at the MAP (Mackay, 1992),

$$P = -\nabla \nabla_{\theta} \mathcal{L}_{\hat{\theta}}. \quad (3)$$

Calculating and inverting  $P$  are the central steps in performing Laplace approximation. For high dimensional  $\theta$  – common in deep neural networks – these steps are a prohibitive computational bottleneck even for an approximate posterior. One remedy is further approximation of the Hessian as well, but these may ignore important directions of curvature.

In this paper we propose Hessian-free Laplace (HFL), which directly approximates the uncertainty of the predicted mean in the Laplace approximation without explicitly computing and inverting the Hessian (while still assuming it exists, as in Laplace). Instead, one additional point estimate is required, the *prediction-regularized* MAP, derived from the network objective with a small amount of regularization added. Under the assumptions that the Laplace approximation is used, we find that the rescaled difference in network outputs given by the MAP and the prediction-regularized MAP recovers the Laplace variance.

Our contributions in this paper are as follows:

- We develop a set of novel methods around *regularization-based uncertainty* that targets the pre-

<sup>1</sup>Netflix Research <sup>2</sup>Cornell University. Correspondence to: James McInerney <jmcinerney@netflix.com>, Nathan Kallus <kallus@cornell.edu>.

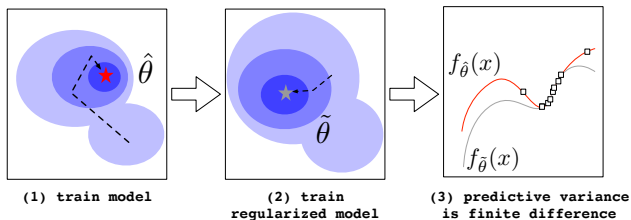


Figure 1. Summary of the regularization-based approach to uncertainty quantification that underlies Hessian-free Laplace. **Step 1:** fit or obtain an existing fit of a predictive model; **step 2:** fit another model using a differently regularized objective (from scratch or warm-started); **step 3:** the difference in predictions of these two models is the predictive variance. In Section 3, we present various types of regularization that make this strategy successful.

dictive variance of linearized Laplace without explicit Hessian calculations. Instead, variance is derived from the change in the MAP when adjusting the regularizer.

- In particular, we present Hessian-free Laplace (HFL), a method that estimates the predictive variance of a network by embedding the prediction of the neural network in the training objective.
- To amortize this procedure over a potentially large number of evaluations, we also develop pre-trained HFL. To our knowledge, this is the first approach to regularization-based uncertainty that scales in the number of evaluations. An illustration of the set of methods considered in this paper is given in Figure 1.

The rest of the paper is organized as follows. In Section 2, we develop the Hessian-free Laplace method. Empirical evaluation is presented in Section 5 before discussing conclusions and future work in Section 6.

## 2. Bayesian Deep Learning with Hessian-Free Laplace

Our starting point is the learning of parameters  $\theta$  of a deep neural network  $f_\theta$  as per Eq. 1 and 2. While the representational power and accuracy of the network may be high, in many applications it is crucial to also quantify the uncertainty of predictions, such as in autonomous vehicles, healthcare, risk-averse recommendations (Kendall & Gal, 2017; Leibig et al., 2017).

Bayesian probability theory provides a framework for analyzing uncertainty in deep learning, referred to as Bayesian deep learning (BDL). As for Bayesian inference in general, the key components are the prior distribution  $p(\theta)$  and likelihood function  $p(y | \theta, x)$  in a family of models indexed by  $\theta$ , and an i.i.d. dataset  $\mathcal{D} = \{(x_i, y_i)\}_{i=1}^n$  assumed to

be collected from a model in this family. The posterior distribution is then derived,

$$p(\theta | \mathcal{D}) = \frac{p(\mathcal{D} | \theta)p(\theta)}{\int p(\mathcal{D} | \theta)p(\theta)d\theta}, \quad (4)$$

and may be flexibly used as the density (or mass) for the expectation of any downstream prediction depending on  $\theta$ , e.g. expectation or variance of predicted mean, as part of a larger simulation involving fitted deep models, or interpreting the variance of weights for different layers of the network. The main evaluations of interest in BDL are the mean  $\mathbb{E}_{p(\theta | \mathcal{D})}[f_\theta(x)]$  and (co)variance  $\text{Var}_{p(\theta | \mathcal{D})}[f_\theta(x)]$  of the prediction for a query vector (or set of query vectors)  $x$ . These will be the focus of our study in this paper.

**Double Intractability** The steps in BDL discussed so far are doubly intractable in the following ways.

- **Model Evidence** For all but the most trivial networks, the integral in the denominator of Eq. 4, (the model evidence) entails a sum over high-dimensional  $\theta$ . Many techniques have been developed to approximate the posterior – the most common being MAP estimation, variational inference, and Markov chain Monte Carlo – and these vary in their scalability and applicability to deep neural nets (Blundell et al., 2015; Ritter et al., 2018). A key desideratum for approximate inference that is often overlooked is the extent to which it is compatible with existing deep learning frameworks and implementations, which may be supported by multiple years of model selection, tuning, and vast training budgets. The MAP point estimate is the most practical in this sense, and is the basis of the Laplace approximation.
- **Posterior Predictive** The posterior predictive  $p(y | \mathcal{D}, x)$  is the expected predictive density, involving complex function  $f_\theta$ , under averages of the approximate posterior, meaning that the integral cannot be further simplified. Monte Carlo estimation using samples from the posterior is used to address this intractability.

**Laplace Approximation** Let  $q$  be the Laplace approximation of the posterior, defined as the second-order Taylor expansion around  $\hat{\theta}$ ,

$$\log q(\theta) = \log p(\hat{\theta} | \mathcal{D}) - \frac{1}{2}(\theta - \hat{\theta})^\top P(\theta - \hat{\theta}), \quad (5)$$

where  $P \hat{=} -\nabla\nabla_\theta \log p(\theta | \mathcal{D})$ . The first derivative does not appear in Eq. 5 because  $\hat{\theta}$  is defined as a local optimum of the posterior, where it exists.

By inspection of Eq. 5, we see that,

$$q(\theta) \propto \exp \left\{ -\frac{1}{2}(\theta - \hat{\theta})^\top P(\theta - \hat{\theta}) \right\} \quad (6)$$

$$\implies q(\theta) = \mathcal{N}(\hat{\theta}, P^{-1}). \quad (7)$$

If precision matrix  $P$  can be calculated and inverted, then the first intractability of approximating the posterior is addressed. In addition, Eq. 7 also provides a closed-form solution to the model evidence, supporting model and hyperparameter selection (MacKay, 1992). We next discuss precision calculation in more detail.

**Precision Matrix** Eq. 7 depends on calculating the covariance matrix, i.e. inverting the precision matrix  $P$  which can be decomposed as,

$$P = -\nabla\nabla_\theta \log p(\theta | \mathcal{D}) \\ = \underbrace{-\nabla\nabla_\theta \log p(\theta)}_{\text{Gaussian prior} \implies \text{scalar matrix}} - \underbrace{\nabla\nabla_\theta \log p(\mathcal{D} | \theta)}_{\text{Hessian } H}. \quad (8)$$

The prior term in Eq. 8 usually takes a simple form, e.g. constant scalar for Gaussian prior, so our focus from this point will be on  $H$ , the Hessian of the *likelihood*.

The Hessian of the likelihood term may be further decomposed as,

$$H = \nabla\nabla_\theta \log p(y | f_\theta(x)) \\ = \underbrace{\nabla_f \log p(y | f_\theta(x))}_{\text{residual}} \nabla\nabla_\theta f_\theta(x) + \\ \underbrace{\nabla\nabla_f \log p(y | f_\theta(x))}_{\text{observation precision}} \nabla\nabla_\theta f_\theta(x) \nabla\nabla_\theta f_\theta(x)^\top. \quad (9)$$

In practice, the precision calculation of the Laplace approximation drops the first term – the network Hessian – in Eq. 9 due to computational constraints. This is known as generalized Gauss-Newton (GGN) and is proportional to the outer product of the network Jacobian (second term in Eq. 9). Beyond expediency, there are two arguments motivating GGN:

1. When fitting highly flexible models, as in BDL, the residual error is expected to be  $\approx 0$ .
2. The residual is a zero-mean random variable uncorrelated with the network Hessian, so the first term is approximately zero as the number of data points grows.

Immer et al. (2021) observed that when GGN is used in approximate inference, it assumes the network takes the form of a generalized linear model. In Laplace, this is equivalent to a local linearization of the network prediction around  $\hat{\theta}$ ,

$$\tilde{f}_\theta(x) \hat{=} f_{\hat{\theta}}(x) + \nabla_\theta f_{\hat{\theta}}(x) \Big|_{\hat{\theta}}^\top (\theta - \hat{\theta}), \quad (10)$$

which experimentally results in more accurate predictions than the original network  $f_{\hat{\theta}}$  when used in the Monte Carlo average for evaluation (Foong et al., 2019). However, the Hessian, even after simplifying with GGN, is still unwieldy or prohibitive to compute, store, and invert for large networks with high dimensional  $\theta$ .

### 3. Hessian-free Laplace (HFL)

Against this background, we target the same mathematical object as the Laplace approximation, requiring the Hessian to exist but avoiding the need to calculate or invert it. To start, notice that an immediate consequence of Eq. 10 is,

$$\tilde{f}_\theta \sim \mathcal{N}(f_{\hat{\theta}}(x), \nabla_\theta f_{\hat{\theta}}(x)^\top P^{-1} \nabla_\theta f_{\hat{\theta}}(x)), \quad (11)$$

where  $\nabla_\theta f_{\hat{\theta}} \hat{=} \nabla_\theta f_\theta \Big|_{\hat{\theta}}$  is used for more compact notation.

This is an instance of the Bayesian delta method (Wasserman, 2006), differing from the classic delta method by the inclusion of the prior term in  $P$  in Eq. 8.

The posterior predictive depends on the form of the observation likelihood function. For regression tasks, Gaussian observation noise with fixed standard deviation  $\sigma$  is the standard, resulting in posterior predictive equal to Eq. 11 plus additional variance term  $\sigma^2$ . For classification tasks, the posterior predictive is non-analytical, requiring Monte Carlo averaging over posterior samples. Notwithstanding the particular form of the posterior predictive distribution, the *epistemic uncertainty* of the network predictions – meaning, the error due to lack of knowledge – is represented by Eq. 11 and has considerable value in active learning, experimental design, and exploration-exploitation.

We set up the prediction-regularized joint distribution as equal to the joint distribution (Eq. 2) with an additional term proportional to the prediction at query point  $x$ ,

$$\mathcal{L}_\theta^{(x,\lambda)} = \sum_{i=1}^n \log p(y_i | f_\theta(x_i)) + \log p(\theta) + \lambda f_\theta(x), \quad (12)$$

for some constant  $\lambda \in \mathbb{R}$ . The prediction-regularized MAP is defined as,

$$\hat{\theta}^{(x,\lambda)} \in \arg_\theta \max \mathcal{L}_\theta^{(x,\lambda)}. \quad (13)$$

**Theorem 3.1.** *The derivative of the prediction under the prediction-regularized MAP w.r.t.  $\lambda$  recovers the variance-covariance term in Eq. 11,*

$$\nabla_\lambda f_{\hat{\theta}^{(x,\lambda)}}(x) \Big|_{\lambda=0} = \nabla_\theta f_{\hat{\theta}}(x)^\top P^{-1} \nabla_\theta f_{\hat{\theta}}(x), \quad (14)$$

assuming  $\hat{\theta}^{(x,\lambda)}$  and  $P^{-1}$  exist, and that  $\mathcal{L}_\theta^{(x,\lambda)}$  is continuously differentiable w.r.t.  $\theta$ .

**Algorithm 1** Hessian-Free Laplace

**Input:** network  $f_\theta$ , fitted MAP  $\hat{\theta}$ , training data  $\mathcal{D}$  of size  $n$ , evaluation input  $x$ , scalar  $\lambda$ , step size schedule  $\gamma(\cdot)$   
 Warm start  $\hat{\theta}^{(x,\lambda)} \leftarrow \hat{\theta}$   
 Initialize step counter  $j = 0$   
**repeat**  
   Sample training example  $(x_i, y_i) \sim \mathcal{D}$   
   Follow stochastic gradient  $\hat{\theta}^{(x,\lambda)} \leftarrow \hat{\theta}^{(x,\lambda)} + n\gamma(j)\nabla_\theta \tilde{\mathcal{L}}_\theta^{(x,\lambda)}(x_i, y_i)$  //Using Eq. 21.  
    $j \leftarrow j + 1$   
**until**  $\hat{\theta}^{(x,\lambda)}$  converges  
**Return:** predictive variance  $\hat{\sigma}_f^2(x) := \frac{1}{\lambda} |f_{\hat{\theta}^{(x,\lambda)}}(x) - f_{\hat{\theta}}(x)|$

*Proof.* Consider the derivative w.r.t.  $\theta$  of the prediction-regularized objective at the optimum,

$$\begin{aligned}
 & \nabla_\theta \mathcal{L}_\theta^{(x,\lambda)} \Big|_{\theta=\hat{\theta}^{(x,\lambda)}} \\
 &= \nabla_\theta \mathcal{L}_\theta \Big|_{\theta=\hat{\theta}^{(x,\lambda)}} + \lambda \nabla_\theta f_\theta(x) \Big|_{\theta=\hat{\theta}^{(x,\lambda)}} \\
 &= 0,
 \end{aligned} \tag{15}$$

by definition in Eq. 12 and by definition of the optimum. Now, differentiate Eq. 15 w.r.t.  $\lambda$ , applying the chain rule and noticing that  $\hat{\theta}^{(x,\lambda)}$  is a function of  $\lambda$ ,

$$\begin{aligned}
 & \nabla_\theta^2 \mathcal{L}_\theta \Big|_{\theta=\hat{\theta}^{(x,\lambda)}} \nabla_\lambda \hat{\theta}^{(x,\lambda)} + \nabla_\theta f_\theta(x) \Big|_{\theta=\hat{\theta}^{(x,\lambda)}} \\
 &+ \lambda \nabla_\theta^2 f_\theta(x) \Big|_{\theta=\hat{\theta}^{(x,\lambda)}} \nabla_\lambda \hat{\theta}^{(x,\lambda)} = 0.
 \end{aligned} \tag{16}$$

Evaluating Eq. 16 at  $\lambda = 0$  eliminates the term involving the Hessian of the output. Since, by assumption, the inverse Hessian of the log joint exists, rearrange the terms,

$$\nabla_\lambda \hat{\theta}^{(x,\lambda)} \Big|_{\lambda=0} = - \left( \nabla_\theta^2 \mathcal{L}_\theta \Big|_{\theta=\hat{\theta}^{(x,0)}} \right)^{-1} \nabla_\theta f_\theta(x) \Big|_{\theta=\hat{\theta}^{(x,0)}} \tag{17}$$

Finally, substituting Eq. 17 into the chain rule expansion of  $\nabla_\lambda f_{\hat{\theta}^{(x,\lambda)}}(x) \Big|_{\lambda=0}$  yields,

$$\begin{aligned}
 & \nabla_\lambda f_{\hat{\theta}^{(x,\lambda)}}(x) \Big|_{\lambda=0} \\
 &= -\nabla_\theta f_\theta(x) \Big|_{\theta=\hat{\theta}}^\top \left( \nabla_\theta^2 \mathcal{L}_\theta \Big|_{\theta=\hat{\theta}} \right)^{-1} \nabla_\theta f_\theta(x) \Big|_{\theta=\hat{\theta}}.
 \end{aligned} \tag{18}$$

This recovers Eq. 14 by substituting with the definition of  $P$  (Eq. 3).  $\square$

A parallel frequentist approach is known as the implicit delta method (Kallus & McInerney, 2022). The relationship in Eq. 14 can also be understood as an application of the implicit function theorem (IFT) by Cauchy, e.g. see (Lorraine et al., 2020) for a modern treatment of IFT.

A corollary of Theorem 3.1 is that detecting the local change in prediction as  $\lambda$  is increased (or decreased) from 0 yields the variance term of the linearized Laplace approximation

in Eq. 11. The local change, i.e. the LHS of Eq. 14, may be calculated by finite differences for some suitably small  $\lambda$ ,

$$\frac{1}{\lambda} (f_{\hat{\theta}^{(x,\lambda)}}(x) - f_{\hat{\theta}}(x)) \Big|_{\lambda \rightarrow 0} \rightarrow \nabla_\lambda f_{\hat{\theta}^{(x,\lambda)}}(x) \Big|_{\lambda=0}. \tag{19}$$

It is natural to consider auto-differentiation to calculate the LHS of Eq. 14. From the fact that the optimum  $\hat{\theta}^{(x,\lambda)}$  also changes with  $\lambda$  it can be seen that auto-differentiation must deal with complex operations on optima and is unlikely to lead to a computational advantage unless used in tandem with additional work-arounds.

Putting it together, the Hessian-free Laplace (HFL) approximation is,

$$\tilde{f}_\theta \sim \mathcal{N} \left( f_{\hat{\theta}}(x), \frac{1}{\lambda} (f_{\hat{\theta}^{(x,\lambda)}}(x) - f_{\hat{\theta}}(x)) \right), \tag{20}$$

and differs from linearized Laplace (Eq. 11) by the lack of an explicit Hessian. It is apparent by this comparison that HFL trades the computational and storage expense of dealing with the Hessian for that of a point-wise approximation for each query  $x$ . There are strong arguments in favor of the latter. First, for suitably small  $\lambda$ , the prediction-regularized MAP is close to the MAP for any choice of  $x$ , and so relatively inexpensive to obtain with stochastic gradient descent. By comparison, matrix inversion takes  $\mathcal{O}(K^3)$  computations in the number of network parameters  $K$ . Second, HFL sidesteps the issue of which Hessian approximation to use, a problem analogous to hyperparameter selection in that it depends on several factors including network architecture, likelihood function, and dataset. The approach is summarized in Algorithm 1 and uses the stochastic objective,

$$\tilde{\mathcal{L}}_\theta^{(x,\lambda)}(x_i, y_i) = \log p(y_i | f_\theta(x_i)) + \frac{1}{n} \log p(\theta) + \frac{\lambda}{n} f_\theta(x), \tag{21}$$

for training example  $(x_i, y_i)$ , or an average over a minibatch.

### 3.1. Pre-Training Hessian-Free Laplace

HFL targets the same predictive variance-covariance as the Laplace approximation. However, when evaluating the uncertainty of many predictions, the requirement to fine-tune

**Algorithm 2** Pre-Training Hessian-Free Laplace

**Input:** network  $f_\theta$ , fitted MAP  $\hat{\theta}$ , training data  $\mathcal{D}$  of size  $n$ , evaluation inputs  $\{\hat{x}_{m=1}^M\}$ , scalar  $\lambda$ , step size schedule  $\gamma(\cdot)$   
 Warm start  $\hat{\theta}^{(\hat{r}, \lambda)} \leftarrow \hat{\theta}$   
 Initialize step counter  $j = 0$   
**repeat**  
   Sample training example  $(x_i, y_i) \sim \mathcal{D}$   
   Follow gradient  $\hat{\theta}^{(\hat{r}, \lambda)} \leftarrow \hat{\theta}^{(\hat{r}, \lambda)} + n\gamma(j)\nabla_\theta \mathcal{L}_i$  //Choose  $\mathcal{L}_i$  from Eq. 25, 27, 28, 29, or 31.  
    $j \leftarrow j + 1$   
**until**  $\hat{\theta}^{(\hat{r}, \lambda)}$  converges  
**Return:** predictive variance function  $\hat{\sigma}_f^2(x) := \frac{1}{\tilde{\lambda}} |f_{\hat{\theta}^{(\hat{r}, \lambda)}}(x) - f_{\hat{\theta}}(x)|$  (or parameter variance  $\hat{\sigma}_\theta^2(x) := \frac{1}{\tilde{\lambda}} |\hat{\theta}^{(\hat{r}, \lambda)} - \hat{\theta}|$ )

to the  $f$ -objective specific to each test point is a bottleneck. In order to scale HFL in the number of test points, we develop a pre-training approach that requires only a single model to represent the  $f$ -regularized parameters for a set of evaluation points.

Pre-training is formulated as follows. Find the regularization term  $\hat{r}$  for a finite set of evaluation inputs  $\hat{\mathbf{x}} = \{\hat{x}_{1:M}\}$  that minimizes the average squared L2 norm error of the corresponding  $f$ -regularized parameters,

$$\hat{r} = \arg_r \min \sum_{m=1}^M \|\hat{\theta}^{(f(x_m), \lambda)} - \hat{\theta}^{(r, \lambda)}\|_2^2, \quad (22)$$

using expanded notation for  $\hat{\theta}^{(\cdot, \lambda)}$  to accommodate different functions in the regularization term. Eq. 22 facilitates the calculation of Eq. 20 using  $\hat{\theta}^{(\hat{r}, \lambda)}$  instead of  $\hat{\theta}^{(f(x), \lambda)}$  for arbitrary  $x$  in the domain of  $f$ .

**Theorem 3.2.** *The optimal regularization term defined by Eq. 22 is  $\hat{r} = \frac{1}{M} \sum_{m=1}^M f(\hat{x}_m)$  when  $\hat{\theta}^{(f(x), \lambda)}$  and  $P^{-1}$  exist and  $\mathcal{L}_\theta^{(f(x), \lambda)}$  is continuously differentiable w.r.t.  $\theta$ .*

*Proof.* Take the derivative of the objective in Eq. 22 w.r.t.  $r$ ,

$$\begin{aligned} & \nabla_r \sum_{m=1}^M \|\hat{\theta}^{(f(x_m), \lambda)} - \hat{\theta}^{(r, \lambda)}\|_2^2 \\ &= \nabla_r \sum_{m=1}^M \|(\hat{\theta}^{(f(x_m), \lambda)} - \hat{\theta}) - (\hat{\theta}^{(r, \lambda)} - \hat{\theta})\|_2^2 \\ &= \nabla_r \sum_{m=1}^M \|P^{-1} \nabla_\theta f(\hat{x}_m) - P^{-1} \nabla_\theta r\|_2^2 \quad (23) \\ &= \sum_{m=1}^M \nabla_r \|P^{-1} (\nabla_\theta f(\hat{x}_m) - \nabla_\theta r)\|_2^2 \\ &= 2(P^{-1})^\top P^{-1} \left( \sum_{m=1}^M (\nabla_\theta f(x_m) - \nabla_\theta r) \right), \quad (24) \end{aligned}$$

using Theorem 3.1 to express the difference in optimal parameters in terms involving the inverse Hessian in Eq. 23.

Finally, set the derivative in Eq. 24 to zero and solve for  $r$ , the unique minimizer of the objective (up to a constant that does not depend on  $\theta$ ).  $\square$

A stochastic optimization algorithm for pre-training HFL is given in Algorithm 2, with objective,

$$\mathcal{L}_i = \log p(y_i | f_\theta(x_i)) + \frac{1}{n} \log p(\theta) + \frac{\lambda}{nM} \sum_{m=1}^M f_\theta(\hat{x}_m). \quad (25)$$

This conceptually simple procedure avoids the need to explicitly calculate the Hessian by optimizing one parameter vector  $\hat{\theta}^{(\hat{r}, \lambda)}$ . The evaluation points may be the training dataset, or a specific test set which may be under dataset shift or require out-of-distribution (OOD) prediction.

There are four noteworthy variants based on this pre-training approach that we discuss next. Each can be used in the gradient update step of Algorithm 2, though their applicability varies, as we will discuss.

**Absolute-Valued Regularizer** HFL can be reformulated to absorb a sign term into  $\lambda$  that depends on the sign of the output function by defining,

$$\tilde{\lambda} = \lambda(-1)^{\mathbb{I}[f_\theta(x) < 0]}, \quad (26)$$

where  $\mathbb{I}[c]$  is the indicator function that evaluates to 1 when the condition  $c$  is true and to 0 otherwise. Equivalently, we can use the absolute values of both the HFL regularizer and predictive variance. This leads to the pre-training objective,

$$\mathcal{L}_i^{(AV)} = \log p(y_i | f_\theta(x_i)) + \frac{1}{n} \log p(\theta) + \frac{\lambda}{nM} \|f_\theta(\hat{\mathbf{x}})\|_1, \quad (27)$$

where the final term in Eq. 27 is the (rescaled) sum of absolute values of the function applied to the  $M$  evaluation inputs.

**In-Sample Pre-Training & Data Augmentation** When the train and test data distributions are the same, the mini-batches sampled to optimize the log joint probability of the

model may also be used to regularize it, giving rise to the single-sample stochastic gradient,

$$\mathcal{L}_i^{(\text{IS})} = \log p(y_i | f_\theta(x_i)) + \frac{\lambda}{n} |f_\theta(x_i)| + \frac{1}{nM} \log p(\theta). \quad (28)$$

Furthermore, when the likelihood is Gaussian, the extra term can be absorbed into the likelihood. In particular, completing the square in Eq. 28, by pulling the term  $\frac{\lambda\sigma^2}{nM} (\frac{\lambda\sigma^2}{2nM} - y_i)$  from a constant that does not depend on  $\theta$ , yields the objective,

$$\mathcal{L}_i^{(\text{DA})} = \log \mathcal{N}\left(y_i + \frac{\tilde{\lambda}}{nM} \sigma^2 \mid f_\theta(x_i), \sigma^2\right) + \frac{1}{n} \log p(\theta), \quad (29)$$

for observation variance hyperparameter  $\sigma^2$ . Under the common Gaussian likelihood assumption, Eq. 29 implies that pre-trained HFL is performed by data augmentation, without requiring *any* adjustment to the model architecture or training procedure.

**Parameter Uncertainty Quantification** The same pre-training approach also enables parameter uncertainty quantification by finding the regularizer  $\hat{t}$  that minimizes the average squared L2 norm over the  $K$  dimensions of parameters,

$$\hat{t} = \arg_t \min \sum_{k=1}^K \|\hat{\theta}^{(t, \lambda)} - \hat{\theta}^{(k, \lambda)}\|_2^2. \quad (30)$$

Theorem 3.2 applies to Eq. 30 in combination with absolute value regularization to provide the pre-training objective,

$$\mathcal{L}_i^{(\text{PU})} = \log p(y_i | f_\theta(x_i)) + \frac{1}{n} \log p(\theta) + \frac{\lambda}{nM} \|\theta\|_1, \quad (31)$$

which corresponds to a set of sparsity-inducing Laplace priors over the weights. Thus, when used in concert with a Laplace log prior  $\log p(\theta)$ , the regularization term for HFL is absorbed, with  $\lambda$  perturbing the precision parameter. In this case, it is particularly convenient to implement HFL for parameter uncertainty, as one needs only to adjust the strength of the existing regularizer and use,

$$\hat{\sigma}_\theta^2(x) := \frac{1}{\lambda} |\hat{\theta}^{(\hat{t}, \lambda)} - \hat{\theta}|, \quad (32)$$

as the parameter variance.

## 4. Related Work

The Laplace approximation was first formulated in BDL for small-scale neural networks (MacKay, 1992). Since then,

larger architectures have necessitated Hessian approximations, including Gauss-Newton (Foresee & Hagan, 1997) and Kronecker factorization that places a block diagonal structure on the covariate in line with assumed independence between the layers of a network (Martens & Grosse, 2015).

In recent years, with the aforementioned scalable approximations and renewed appreciation of the advantages of Laplace as a *post-hoc* uncertainty method (Daxberger et al., 2021), a number of new directions were addressed, including relating neural network loss functions to Gaussian process inference (Khan et al., 2019) and exploring the advantages of locally linearized Laplace in out-of-distribution evaluation (Foong et al., 2019). Underfitting in Laplace (Lawrence, 2001) is mitigated in the GGN approximation by switching to the generalized linear model implied by the local linearization (Immer et al., 2021).

Owing to the ubiquity of the Hessian of the objective and its computational demands, approaches to avoiding its direct evaluation are developed in areas of research distinct of Laplace. In particular, Hessian-free optimization uses the conjugate gradient method to iteratively update a matrix-vector product as part of an inner loop in Newton’s method second-order optimization (Martens & Sutskever, 2011; Pearlmutter, 1994).

## 5. Experiments

We explore four data generating distributions designed to test both in-distribution inference and extrapolation to “in-between” uncertainty (Foong et al., 2019),

- **Quadratic-Uniform** Draw 32 data points  $x \sim \mathcal{N}(0, 1)$  and let  $y = \frac{1}{10}x^2 - \frac{1}{2}x + 5 + \frac{1}{10}\epsilon$ , where  $\epsilon \sim \mathcal{N}(0, 1)$ .
- **Quadratic-Inbetween** Draw 16 data points  $x \sim \text{Uniform}(-2, -\frac{1}{2})$  and 16 data points  $x \sim \text{Uniform}(\frac{4}{5}, \frac{5}{2})$ , using the same response distribution as Quadratic-Uniform.
- **Sin-Uniform** Sample 160 data points  $x \sim \text{Uniform}(-\frac{3}{2}, \frac{23}{20})$  and let  $y = -\sin(3x - \frac{3}{10}) + \frac{1}{10}\epsilon$ , where  $\epsilon \sim \mathcal{N}(0, 1)$ .
- **Sin-Inbetween** Fix 160 data points evenly spaced in ranges  $[-1.5, -0.7]$  and  $[0.35, 1.15]$  and let use the same response as Sin-Uniform.

A feedforward neural network is used with 50 hidden units and tanh activations to ensure that the Hessian exists, and optimized using Adam (Kingma & Ba, 2017) with a learning rate of 0.005. Further experimental details are given in Appendix A. Four methods to quantifying the epistemic uncertainty of the network are compared,

## Hessian-Free Laplace in Bayesian Deep Learning

	Datasets							
	Quadratic		Quadratic-Inbetween		Sin		Sin-Inbetween	
	In-Distribution	OOD	In-Distribution	OOD	In-Distribution	OOD	In-Distribution	OOD
<i>Full Hessian</i>	PICP: 0.9375 CRPS: 0.003156 NLL: -23.924	PICP: 0.9556 CRPS: 0.009017 NLL: -38.027	PICP: 0.9688 CRPS: 0.003797 NLL: -23.290	PICP: 0.8667 CRPS: 0.003331 NLL: -24.538	PICP: 1.0000 CRPS: 0.04666 NLL: -75.764	PICP: 0.8625 CRPS: 0.07498 NLL: 26.004	PICP: 1.0000 CRPS: 0.04486 NLL: -73.178	PICP: 0.9250 CRPS: 0.06022 NLL: 10.029
GGN	PICP: 0.9375 CRPS: 0.003762 NLL: -23.790	PICP: 0.9556 CRPS: 0.007771 NLL: -38.751	PICP: <b>0.9688</b> CRPS: 0.003992 NLL: <b>-23.135</b>	PICP: 0.8444 CRPS: 0.0008355 NLL: -23.504	PICP: 1.0000 CRPS: 0.04652 NLL: -76.025	PICP: 0.8250 CRPS: 0.05493 NLL: 101.6	PICP: 1.0000 CRPS: 0.04482 NLL: -73.260	PICP: 0.8875 CRPS: 0.04302 NLL: 24.903
Eigen. Approx.	PICP: 0.9375 CRPS: 0.003760 NLL: -23.789	PICP: <b>0.9556</b> CRPS: 0.007705 NLL: <b>-38.760</b>	PICP: 0.9688 CRPS: 0.003566 NLL: -23.098	PICP: 0.8444 CRPS: 0.0001922 NLL: -22.893	PICP: <b>1.0000</b> CRPS: <b>0.04605</b> NLL: <b>-77.027</b>	PICP: 0.8250 CRPS: <b>0.05364</b> NLL: 109.7	PICP: <b>1.0000</b> CRPS: <b>0.04454</b> NLL: <b>-73.785</b>	PICP: 0.8875 CRPS: <b>0.04208</b> NLL: 27.112
HFL (this paper)	PICP: <b>0.9375</b> CRPS: <b>0.002347</b> NLL: <b>-23.899</b>	PICP: 0.9333 CRPS: <b>0.006976</b> NLL: -38.440	PICP: 0.8750 CRPS: <b>0.001782</b> NLL: -22.571	PICP: <b>0.8444</b> CRPS: <b>4.735e-05</b> NLL: <b>-23.676</b>	PICP: 1.0000 CRPS: 0.04691 NLL: -75.245	PICP: <b>0.8375</b> CRPS: 0.06397 NLL: <b>45.483</b>	PICP: 1.0000 CRPS: 0.05016 NLL: -63.218	PICP: <b>0.9250</b> CRPS: 0.06301 NLL: <b>22.915</b>

Table 1. Uncertainty quantification performance across datasets and methods. Top performing metrics, as defined in Section 5, are in bold, with ties broken by the other metrics. *Full Hessian* is a benchmark comparison that is intractable at scale.

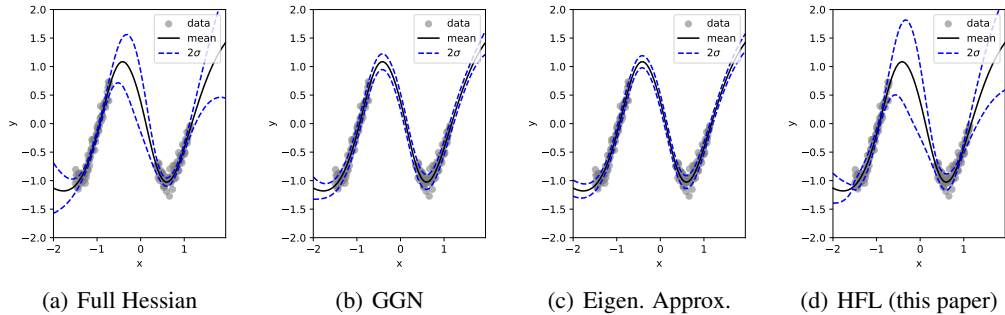


Figure 2. Illustration of epistemic uncertainties of the predicted mean for the Sin-Inbetween OOD task.

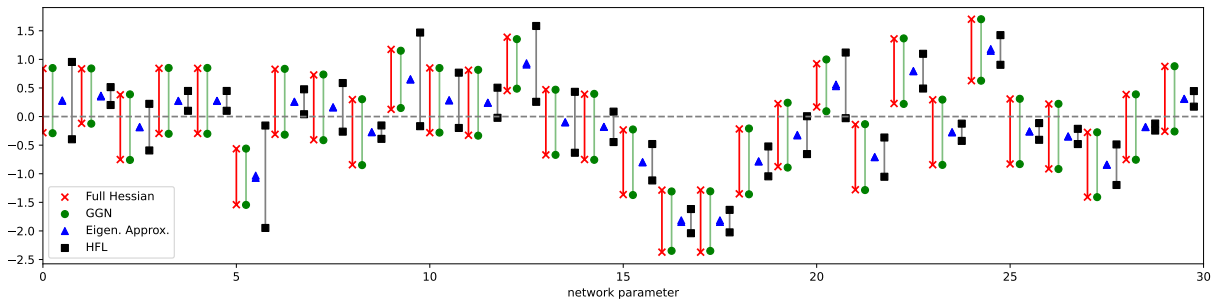


Figure 3. The uncertainty ranges of a random subset of 30 parameters of the neural network indicate that many parameters include 0 in their intervals. HFL recovers much of the structure of these uncertainties via additional regularization of the network parameters in the objective function.

- **Exact Hessian** using Eq. 8 and both terms in the likelihood Hessian (Eq. 9).
- **GGN** using Eq. 8 with only the second term in likelihood Hessian (Eq. 9).
- **Eigenvector approximation** of the GGN for  $P^{-1} \approx A\Lambda^{-1}A^T$  using the top  $k$  eigenvectors  $A$  of  $P$  (with corresponding eigenvalues  $\Lambda$ ) where  $k =$

$\log_e(\dim(\theta))$  rounded to the nearest positive integer. The GGN is chosen because it only makes sense to use the eigenvector approximation when the Hessian is large.

- **HFL** (this paper), using Algorithm 2.

The metrics used to evaluate uncertainty performance are,

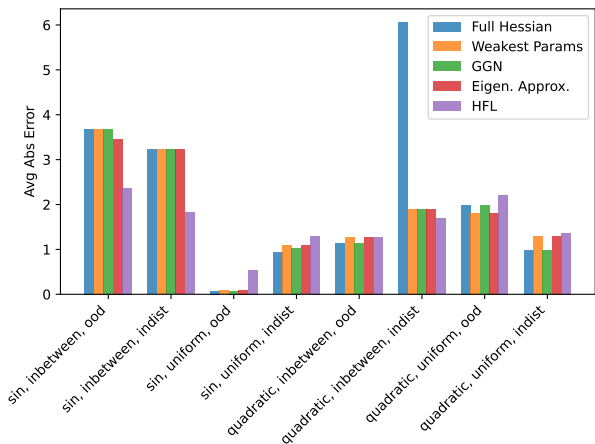


Figure 4. Absolute errors in predicted means for all the tasks with networks with added sparsity using the uncertainty quantification methods.

- **Prediction interval coverage probability (PICP)** assesses calibration by evaluating how well prediction intervals cover the observed values. It is calculated as the proportion of times the held-out observed value  $y$  falls within the 95% confidence interval of the predicted observations (closer to 0.95 is better).
- **Continuous Ranked Probability Score (CRPS)** is a generalization of the Brier score for continuous outcomes, measuring the difference between the CDF of the predicted observations and the CDF of the observed response variable (smaller is better).
- **Negative log likelihood (NLL)** evaluates the negated predicted log likelihood of the held out observations (smaller is better).

The results of the evaluations are summarized in Table 1. We find that HFL performs commensurately with other approximations, and indeed the full Hessian, despite taking a significantly different approach. In particular, in several cases it achieves the best out-of-distribution (OOD) performance, likely due to its ability to avoid the GGN assumption that ignores an important part of the curvature around the MAP. To illustrate this point, we plot the predicted mean output for the methods on the Sin-Inbetween OOD task in Figure. 2. There is a noticeable difference to the GGN and eigenvector approximation, implying that in practice the residual of the loss may not be close to zero.

We also evaluated the parameter regularization approach given in Eq. 31. Figure 3 shows the 1 standard deviation interval about the predicted mean under the various methods. Recall that HFL for parameter uncertainty requires only to

apply a small amount of additional L1 regularization to the parameters. Nonetheless, the intervals indicated often align with those requiring full Hessian inversion. These parameter uncertainties may be used for model introspection. As an example, we considered the task of adding sparsity to a network, setting parameters to 0 when their uncertainty intervals overlap with 0. The mean absolute errors of the resulting predictions are shown in Figure 4. HFL does competitively, particularly for in-between uncertainty. An outlier result is the absolute error of the full Hessian in the Quadratic-Inbetween in-distribution task. This was due to mis-selecting an entire group of units to be set to 0, greatly impacting the shape of the predicted function.

**Limitations** HFL is subject to the same assumptions and limitations as the Laplace approximation, primarily, that it is a local method centered around the optimum of the joint distribution and the curvature is evaluated at one location (ignoring any other modes). In practice, early stopping and highly overparameterized networks break these assumptions, reducing the quality of the uncertainties. In addition, pre-trained HFL introduces error in the set of evaluation points embedded in the regularized objective, though this has so far been observed to be mild in practice.

## 6. Conclusions & Future Work

In this paper we developed HFL, a set of approaches to Laplace approximation without explicit Hessian evaluation and inversion. Instead, two point estimates are used, the usual MAP estimate and a regularized form of the MAP. Theoretical and experimental evidence supports this method both in terms of accuracy of predictive variance and the favorable scaling properties in the number of parameters of the model. Future work is required to investigate the role of these approximations in architectures of greater complexity as well as their potential role in directing exploration, experimentation, training data selection, and model introspection.

## References

Blundell, C., Cornebise, J., Kavukcuoglu, K., and Wierstra, D. Weight uncertainty in neural networks. In *International Conference on Machine Learning*, pp. 1613–1622, 2015.

Daxberger, E., Kristiadi, A., Immer, A., Eschenhagen, R., Bauer, M., and Hennig, P. Laplace redux-effortless Bayesian deep learning. *Advances in Neural Information Processing Systems*, 34:20089–20103, 2021.

Foong, A. Y., Li, Y., Hernández-Lobato, J. M., and Turner, R. E. 'In-between' uncertainty in Bayesian neural networks. *arXiv preprint arXiv:1906.11537*, 2019.

- Foresee, F. D. and Hagan, M. T. Gauss-Newton approximation to Bayesian learning. In *Proceedings of international conference on neural networks (ICNN'97)*, volume 3, pp. 1930–1935. IEEE, 1997.
- Immer, A., Korzepa, M., and Bauer, M. Improving predictions of Bayesian neural nets via local linearization. In *International Conference on Artificial Intelligence and Statistics*, pp. 703–711. PMLR, 2021.
- Kallus, N. and McInerney, J. The implicit delta method. *Advances in Neural Information Processing Systems*, 35: 37471–37483, 2022.
- Kendall, A. and Gal, Y. What uncertainties do we need in Bayesian deep learning for computer vision? *Advances in Neural Information Processing Systems*, 30, 2017.
- Khan, M. E. E., Immer, A., Abedi, E., and Korzepa, M. Approximate inference turns deep networks into Gaussian processes. *Advances in neural information processing systems*, 32, 2019.
- Kingma, D. P. and Ba, J. Adam: A method for stochastic optimization. *arXiv preprint arXiv:1412.6980*, 2017.
- Lawrence, N. D. *Variational inference in probabilistic models*. PhD thesis, 2001.
- Leibig, C., Allken, V., Ayhan, M. S., Berens, P., and Wahl, S. Leveraging uncertainty information from deep neural networks for disease detection. *Scientific Reports*, 7(1): 17816, 2017.
- Lorraine, J., Vicol, P., and Duvenaud, D. Optimizing millions of hyperparameters by implicit differentiation. In *International Conference on Artificial Intelligence and Statistics*, pp. 1540–1552. PMLR, 2020.
- MacKay, D. J. Bayesian interpolation. *Neural Computation*, 4(3):415–447, 1992.
- Mackay, D. J. Bayesian methods for adaptive models. *Doctoral Thesis, California Institute of Technology*, 1992.
- Martens, J. and Grosse, R. Optimizing neural networks with Kronecker-factored approximate curvature. In *International conference on machine learning*, pp. 2408–2417. PMLR, 2015.
- Martens, J. and Sutskever, I. Learning recurrent neural networks with Hessian-free optimization. In *Proceedings of the 28th international conference on machine learning (ICML-11)*, pp. 1033–1040, 2011.
- Pearlmutter, B. A. Fast exact multiplication by the Hessian. *Neural computation*, 6(1):147–160, 1994.
- Ritter, H., Botev, A., and Barber, D. A scalable Laplace approximation for neural networks. In *6th International Conference on Learning Representations, ICLR 2018-Conference Track Proceedings*, volume 6. International Conference on Representation Learning, 2018.
- Wasserman, L. *All of nonparametric statistics*. Springer, 2006.

## A. Further Experimental Details

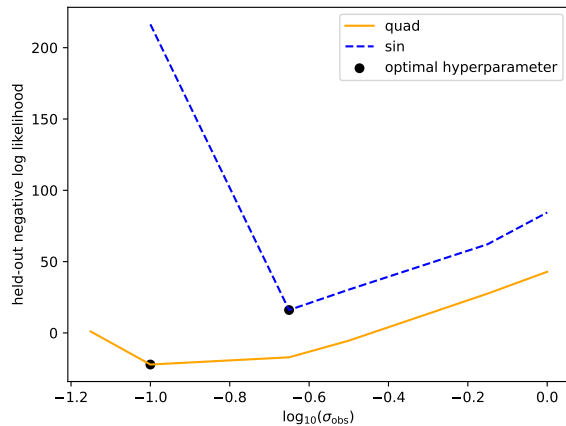


Figure 5. Hyperparameter sweeps for observational variance.

For both the quadratic and sin datasets, the observational variance hyperparameter was selected through grid search over the set  $\{0.005, 0.01, 0.05, 0.1, 0.5, 1.0\}$  minimizing negative log likelihood for a held-out validation set of equal size to the training dataset. The results are summarized in Figure 5, with the optimal hyperparameter chosen indicated by a marker. The prior variance was fixed at 3.0, which was the minimum value to the nearest 0.1 for which the Hessian was sufficiently conditioned across all tasks to allow for inversion.